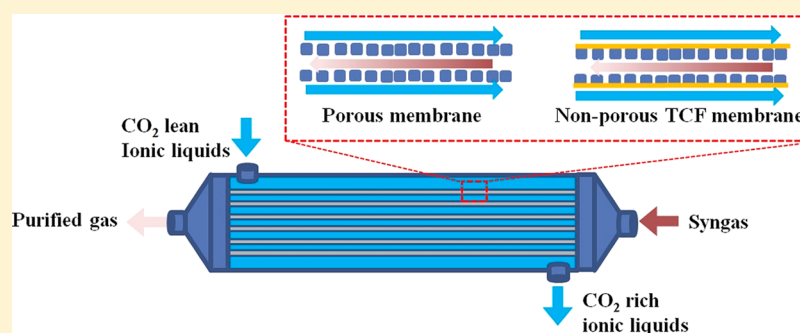# Precombustion CO_2 Capture in Polymeric Hollow Fiber Membrane Contactors Using Ionic Liquids: Porous Membrane versus Nonporous Composite Membrane

Zhongde Dai, Luca Ansaloni, and Liyuan Deng*

Department of Chemical Engineering, Norwegian University of Science and Technology (NTNU), Trondheim 7491, Norway

ABSTRACT: In the present work, membrane contactors using both porous and nonporous polymeric hollow fiber membranes with ionic liquids as absorbent were developed for precombustion CO_2 capture at elevated temperature and pressures. 1-Butyl-3-methylimidazolium tricyanomethanide [Bmim][TCM] was selected as the ILs absorbent. The compatibility and stability of six different polymeric membranes were evaluated, while the porous PTFE membrane and nonporous Teflon-PP composite membrane were considered to be the most suitable membranes for this application. Both membrane configurations were tested and showed comparable separation performances: CO_2 flux values of 4.86×10^{-4} and 4.75×10^{-4} mol m^{-2} s^{-1} were obtained for the porous PTFE and nonporous Teflon-PP membrane contactor at 20 bar with a gas flow rate of 200 mL min^{-1}, respectively. The Teflon-PP composite membrane exhibited better stability as compared to the porous PTFE membrane in a 14 day test.

1. INTRODUCTION

CO_2 capture and storage (CCS) has been regarded as one of the most promising options to utilize fossil fuels without a significant influence on climate change.[1] CO_2 can be separated after the combustion process (postcombustion) or before feeding the syngas to the gas turbine (precombustion). Postcombustion CO_2 capture separates CO_2/N_2 mixtures (5−15 vol % CO_2) at near atmospheric pressure, whereas the precombustion process separates CO_2/H_2 mixtures with a higher CO_2 concentration (~45 vol %) at an elevated pressure (15−20 bar) and temperature (190−210 °C). In view of the larger CO_2 concentration, the precombustion capture is more efficient than postcombustion, but the severe operating conditions make the separation process more complicated. In the past few years, many different technologies have been developed for CO_2 capture from syngas, including chemical and physical absorption, solid adsorption, and membrane separation.[2] Membrane absorption is an emerging technology that combines the advantages of membrane and absorption. The main advantages of a membrane absorption process include large gas−liquid interfacial area, operation flexibility, no flooding and/or foaming phenomena, small footprint, and easy up-scaling.[3−5]

The absorbent selection for a CO_2 capture membrane contactor is critical, and various aspects need to be considered, such as good thermal and chemical stability, low viscosity, low corrosion rate, high CO_2 solubility, and selectivity over other gaseous species. In the past few years, a large number of CO_2 absorbents have been tested in membrane contactors for flue gas purification.[6,7] So far, amine-based aqueous solvents have been mostly reported for good CO_2 separation performances, mainly due to their larger cyclic capacities.[8−11] However, the use of amine-based solvents for precombustion operating conditions is threatened by their high volatility, as it causes large solvent loss, a large degradation rate at high temperatures, and a high corrosion rate of metallic pipes and tanks.[12] In this regard, ionic liquids (ILs) have also been studied as promising CO_2 capture absorbents in the past decade[13] due to their unique properties such as negligible volatility, high CO_2 solubility, superior thermal stability, and tailorable structures. The good thermal stability and low volatility of ILs also ensure their application with nearly no solvent loss even at elevated temperatures.[14] Despite these facts, there are only a handful of reports on membrane absorption processes using ILs absorbents for gas separation.[15−22] Most of the reported

literature employed porous membranes, and the membrane contactor was operated under mild conditions (~1 bar, close to room temperature). In 2009, Albo et al. first applied ILs into a membrane contactor and developed a "zero solvent emission" membrane absorption process based on 1-ethyl-3-methylimidazolium ethylsulfate [Emim][EtSO$_4$] and commercially available PP membrane for postcombustion CO_2 capture.[19] Afterward, more IL-based absorbents were studied in membrane absorption processes for CO_2 capture, such as 1-ethyl-3-methylimidazolium acetate [Emim][Ac],[18] 1-butyl-3-methyl-imidazolium tetrafluoroborate ([Bmim][BF$_4$]), 1-(3-aminopropyl)-3-methyl-imidazolium tetrafluoroborate ([apmim][BF$_4$]),[22] and 1-butyl-3-methylimidazolium dicyanamide [Bmim][DCA].[23] Sirkar et al. studied the possibility of using ILs in a membrane contactor for precombustion CO_2 capture at elevated temperature and pressures. This process design is similar to a pressure swing adsorption: there is no flow or recirculation of the liquid phase in the membrane contactor.[17]
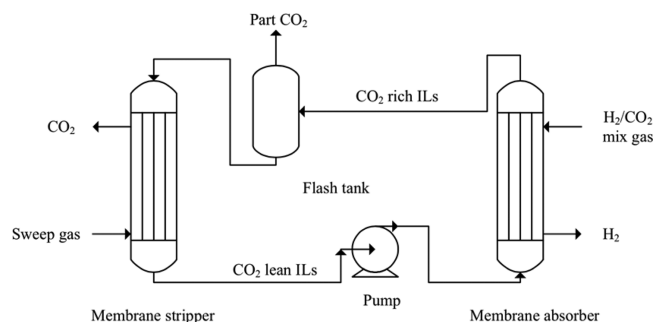
The membranes in the majority of the literature concerning membrane contactors are porous with no gas selectivity,[3] typically made of hydrophobic materials such as polyethylene (PE), polypropylene (PP), polyvinylidenefluoride (PVDF), and polytetrafluoroethylene (PTFE).[3] Ideally, the membrane pores should be gas-filled to ensure a high overall mass transfer coefficient. However, pore-wetting starts gradually and becomes more serious with time, lowering the efficiency of the separation process in the long term.[24] Indeed, due to the lower gas diffusivity in a solvent-filled pore (the gas diffusion coefficient through fluids changes from the order of 10^{-1} cm^2 s^{-1} in gas to the order of 10^{-5} cm^2 s^{-1} in liquids), membrane wetting generates a large increase in the overall mass transfer resistance.

Several criteria must be fulfilled for the selection of a suitable porous material in a membrane contactor, including good chemical, thermal, and mechanical stability, sharp pore size distribution, high porosity, and a high contact angle with the absorbent. A successful approach to eliminate the occurrence of pore wetting is the use of a nonporous composite membrane with a thin dense top layer as a gas/liquid interface in the contactor.[25−27] By placing the dense layer in contact with the liquid phase, liquid penetration in the pores can be prevented,[25] and the possibility of gas bubbling into the solvent phase and solvent entrainment into the gas phase can be also reduced. Nevertheless, the dense layer provides an additional mass transfer resistance to the CO_2 transport from the gas to the liquid phase, and thus materials with large CO_2 permeability are preferred to minimize the membrane impact on the overall mass transfer coefficient. High free volume polymers such as PTMSP, PIM-1, and PMP are the most commonly reported materials in this case due to their extremely high CO_2 permeability.[25,28] However, these membranes are subjected to significant aging, and their performance reduces quickly over time.[29] Fluorinated polymers such as Teflon AF 1600 and Teflon AF 2400 have also been employed to prepare thin film composite membranes and been applied in membrane contactors due to their chemical and thermal stability, the relatively high CO_2 permeability, and the stable long-term performances.[25,28] Because of the high active membrane area per unit volume, hollow fibers membranes are most commonly used in membrane contactors. Furthermore, this surface area-to-volume ratio varies inversely with fiber diameter increase,

whereby a hollow fiber membrane with a smaller diameter is preferred.

A closed loop, pressure swing membrane contactor process for precombustion CO_2 capture has been developed in our group, aiming at the purification of hydrogen in a CO_2/H_2 mixture coming from the second water−gas shift reaction (as shown in Scheme 1). In this process, H_2 is purified in the

Scheme 1. Schematic Representative of the Novel Membrane Contactor for Precombustion CO_2 Capture[a]
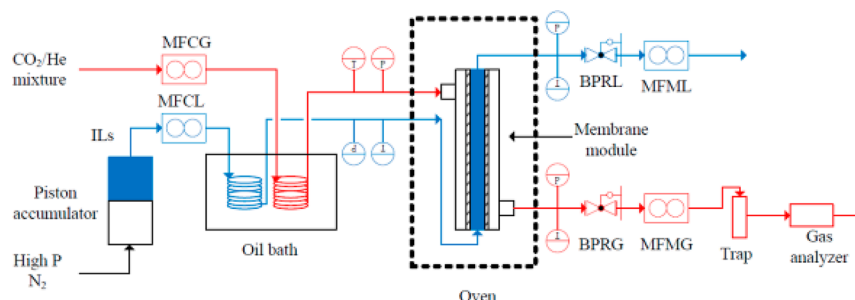

[a]Reproduced with permission from ref 30. Copyright 2016 Elsevier.

absorber under elevated pressure conditions (i.e., 20 bar), and CO_2 is selectively absorbed in the IL phase. Subsequently, the CO_2-rich IL absorbent is sent to a flash tank to partially remove the absorbed CO_2 and then to a membrane desorber at a reduced pressure and higher temperature to complete the absorbent regeneration. Finally, the CO_2 lean IL stream is pumped into the membrane absorber again, and the whole process forms a closed loop. This design combines the advantages of pressure swing absorption (PSA), temperature swing absorption (TSA), and a membrane contactor.

The present work focuses on the membrane absorption step of the process under elevated temperature (80 °C) and pressure (20 bar). Precombustion conditions have a temperature much higher than 80 °C. However, 80 °C was chosen in this work due to engineering considerations. As [Bmim]-[TCM] is a physical absorbent, the CO_2 solubility in [Bmim][TCM] decreases when temperature increases, which reduces the CO_2 cyclic capacity and thus increases the operating energy consumption. In addition, [Bmim][TCM] presents reasonable viscosity at this temperature, while at a lower temperature, the viscosity is too high and not practical. Moreover, ILs have been proven as good solvents for many polymers and organic compounds, which may gradually attack or swell the membrane or sealing materials in the membrane module, especially at high temperatures; it is in general more expensive and challenging to maintain membrane and sealing materials for a membrane contactor at higher temperatures.

[Bmim][TCM] was selected as the absorbent due to its relatively low viscosity, good thermal stability, and high CO_2 absorption capacity.[31] Initially, a compatibility analysis was carried out by considering four different porous hollow fiber membranes (polyvinylidene fluoride (PVDF), polytetrafluoroethylene (PTFE), polyazole, and polypropylene (PP)), and two thin film composite membranes (polymethylpentene (PMP) composite and Teflon AF 2400-PP composite membrane). These membrane materials were characterized in terms of their chemical stability, thermal stability, and contact angle with respect to the liquid phase. Moreover, the separation performances of two selected membranes (porous PTFE

Scheme 2. Schematic Representation of the Experimental Membrane Contactor Setup Used for CO$_2$/He Separation[a]

[a]MFCG and MFCL represent the mass flow controller for the gas and the liquid stream, BPRG and BPRL denote the backpressure regulator for gas and liquid, and MFMG and MFML are the mass flow meter for gas and liquid, respectively. P and T represent the pressure sensor and temperature sensor.

membrane and nonporous Teflon-PP composite membrane) were investigated. The effects of the operating pressure, gas flow rate, and long-term stability on the overall CO$_2$ mass transfer coefficient were studied. Finally, the separation performances by using the selected porous and nonporous membranes were compared with respect to the CO$_2$ flux and long-term stability.

2. EXPERIMENTAL SECTION

2.1. Materials. The [Bmim][TCM] was purchased from Iolitech (Germany) and used without any further purification. The isopropanol (IPA) was purchased from Sigma-aldrich (Norway) and used without further treatment. The nitrogen (99.99%) and certified gas mixture (45 vol % CO$_2$ in helium balance) cylinders were purchased from AGA (Norway). The high-temperature glue used for sealing the membrane module was purchased from Aremco Products Inc. (U.S.). The Teflon AF 2400 was ordered from Chemours (U.S.), and the Fluorinert FC72 was purchased from Kemi-Intressen AB (Sweden).

The porous PVDF and porous PTFE hollow fiber membrane were kindly provided by Dr. Zhao's group from the Tianjin Polytechnic University. The porous polyazole hollow fiber membrane was kindly offered by Prof. Nunes's group from the King Abdullah University of Science and Technology. The porous PP and the PP-PMP composite membrane were supplied by Membrana GmbH.

2.2. Teflon-PP Membrane Preparation. The Teflon-PP membrane was prepared through a dip-coating procedure. The PP hollow fiber was first soaked in the IPA solution for 10 s to reduce possible coating solution penetration, and then dip-coated in the 0.5 wt % Teflon AF 2400 solution for 10 s. After 10 min, the membrane was coated again with the same Teflon AF 2400 solution for another 10 s. The double coated membrane was left in an ambition condition for at least 24 h, followed by drying the membrane in a vacuum oven at 60 °C for 6 h to remove the residual solvent.

2.3. Materials Characterization. *2.3.1. Chemical Stability Test.* As the proposed test temperature is 80 °C, the chemical stability of the selected membranes was tested by soaking the membranes in [Bmim][TCM] at 100 °C for at least 6 h. The possible morphology changes of the membranes upon the immersion were investigated using a scanning electron microscope (SEM, TM3030 tabletop microscope, Hitachi High Technologies America, Inc.). The samples were sputter coated with a gold nanoparticle layer to ensure good electrical conductivity (coating time = 1.5 min). The backscattered

electron (BSE) signal and an electron beam intensity of 15 kV are used in the SEM study.

2.3.2. Thermal Stability Test. Thermogravimetric analysis (Q500, TA Instruments) was applied to test the thermal properties of the selected membranes. A sample amount of about 10 mg was used with a N$_2$ sweep flow of 60 mL min^{-1} and a heating rate of 10 °C min^{-1}.

2.3.3. Contact Angle Test. A contact angle goniometer (Attension Theta, Biolin scientific) was used to measure the contact angle between the ILs and the selected membranes. A liquid drop with a volume of 3–5 μL was used, and the contact angle was calculated as the average between the left and right contact angles.

2.4. Experimental Setup and Procedure. The separation performances of the membrane contactor were tested in an in-house-made system. The schematic of the setup (see Scheme 2) and a brief description of the operation are given below.

The feed gas mixture (CO$_2$/He 45/55 vol %, helium was used instead of hydrogen because of safety issues) and ILs were fed through the lumen side and shell side, respectively, with a countercurrent configuration. A piston accumulator (Parker, U.S.), instead of a pump, was employed to inject the liquid into the system to avoid fluctuation and to precisely control the operating parameters in a broad range. This device enabled the system to start from a very small flow rate and to maintain a high pressure (up to 20 bar) at a small flow rate (about 10–20 mL min^{-1}). The gas and liquid flow rates were controlled by two mass flow controllers (Bronkhost, The Netherlands). The gas and liquid side feed pressures were controlled by two back-pressure controllers (Swagelok, U.S.) installed downstream with respect to the membrane module, and the pressure could be adjusted between 1 and 20 bar. The gas- and liquid-phase pressures were measured by four digital manometers (Keller, Switzerland). To prevent the liquid from entering the gas analyzer in case of breakthrough of the liquid into the gas phase, the gas-phase outlet was forced through a liquid trap before reaching the analyzer. The membrane module was placed in a ventilated oven with a temperature control from room temperature to 200 °C. Both the liquid and the gas feeds were preheated before being sent to the membrane absorber. The temperatures were detected by two temperature sensors to make sure the feed reached the desired temperature before being sent to the absorber. The compositions of the gas mixture in the feed and in the retentate were analyzed using a gas analyzer (GSM810, SICK AG, Germany).

The CO_2 absorption flux (N_{CO_2}) and overall mass transfer coefficient (K_{exp}) can be calculated by the following equations, respectively:[32]

$$N_{CO2} = \frac{Q_{g,in}c_{g,in} - Q_{g,out}c_{g,out}}{A}$$ (1)

$$N_{CO2} = K_{exp}\Delta C_g$$ (2)

where $Q_{g,in}$ and $Q_{g,out}$ are the inlet and outlet gas flow rates in $m^3 s^{-1}$, respectively; $c_{g,in}$ and $c_{g,out}$ represent the gas-phase CO_2 concentrations in $mol\ m^{-3}$ at the inlet and outlet, respectively, which are calculated using a sour SRK model from Aspen Hysys;[33] A denotes the active membrane area in m^2; and ΔC is the logarithmic mean driving force based on gas-phase concentration, and can be described as

$$\Delta C_g = \frac{c_{g,in} - c_{g,out}}{\ln\left(\frac{c_{g,in}}{c_{g,out}}\right)}$$ (3)

Stage-cut (θ) is calculated as the ratio between the permeate CO_2 mole flow (q_p) and the feed CO_2 mole flow (q_f):

$$\theta = \frac{q_p}{q_f}$$ (4)
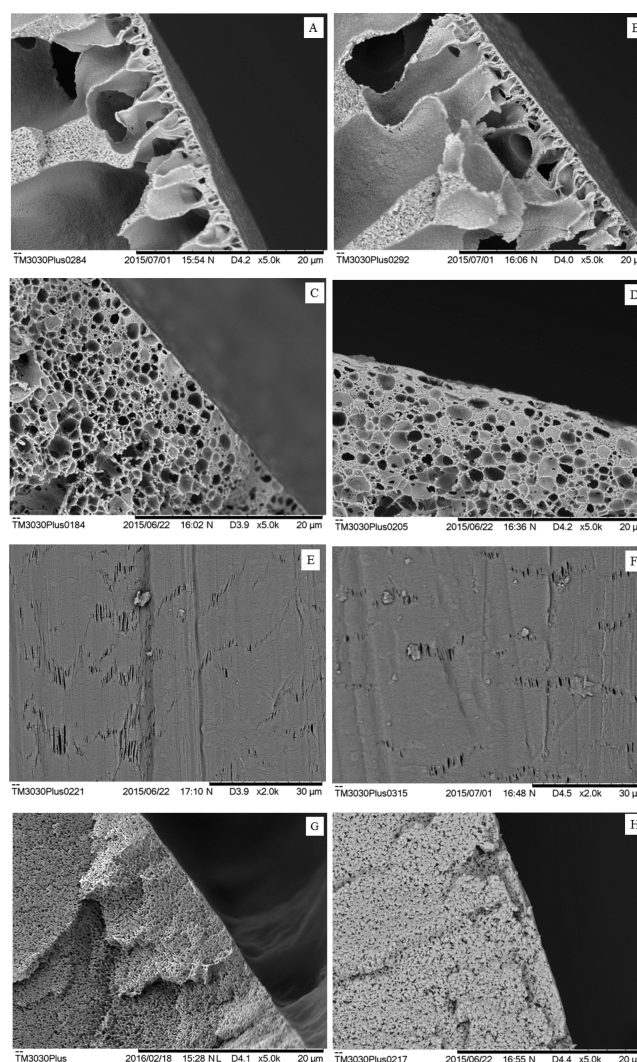
3. RESULTS AND DISCUSSION

3.1. Material Screening for Membrane Selection.
PTFE, PP, and PVDF membranes have been the most reported membranes in membrane contactors for CO_2 capture due to their high hydrophobicity and good stability in aqueous absorbents.[34−36] In this study, PTFE, PP, and PVDF porous hollow fiber membranes were selected as the membrane screening candidates for the designed application. On the basis of the literature study, the porous polyazole hollow fiber membrane was also chosen as a candidate due to its high hydrophobicity and porosity.[37] Two nonporous hollow fiber membranes, Teflon-PP and PMP composite membranes, were also chosen as the nonporous membranes with highly CO_2 permeable dense layers.[38] In this section, the immersion tests were carried out by soaking these membrane samples in [Bmim][TCM] for a determined time, and SEM was used to investigate the possible morphology changes. In addition, contact angle and thermal stability were also tested to identify the most suitable membranes.

3.1.1. Immersion Test. Morphology Study. In view of the target application, the good compatibility/chemical stability at high temperatures is of primary importance for the membrane materials. The six selected membranes were soaked in [Bmim][TCM] and kept at 100 °C for 6 h, which is more severe as compared to the real experimental conditions.

Figure 1A−H presents the morphologies of the four porous hollow fiber membranes (PVDF, polyazole, PTFE, and PP) before and after the immersion tests. For PVDF, polyazole, and PP membranes, cross section was employed. However, due to the superior mechanical strength and relatively large membrane diameter (~200 μm) of the PTFE membrane, it is impossible to break the membrane in liquid nitrogen to prepare the cross section SEM sample; therefore, only surface SEM images were presented. It is clear that no morphological differences can be observed for all four of these porous membranes before and after the immersion. However, a clear change in color took place with PVDF and polyazole membranes during the tests:

Figure 1. PVDF (A,B), polyazole (C,D), PTFE (E,F), and PP (G,H) membrane before (left) and after (right) the immersion tests.
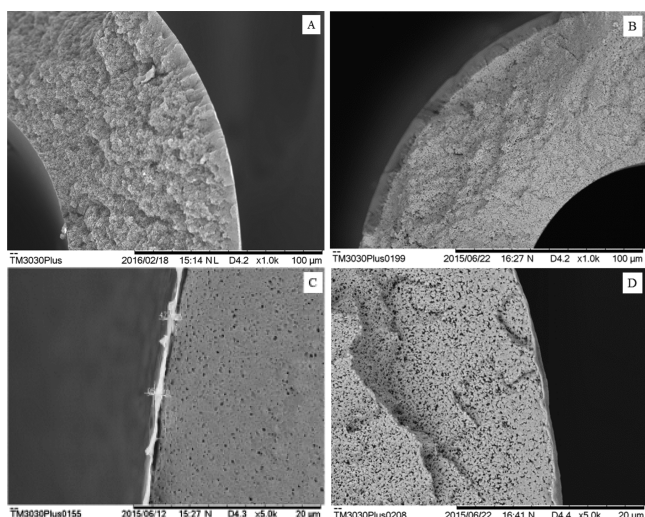
they turned from white to transparent, most likely due to the spontaneous penetration of IL into the membrane pores.

In terms of the porous PTFE and PP membranes, no significant morphology was observed before and after the immersion tests, demonstrating a good chemical stability of the two membranes in [Bmim][TCM]. These two membranes exhibited no color change in the immersion tests, suggesting that no spontaneous penetration of IL occurred.

Figure 2 shows the results obtained for the nonporous PMP composite membrane and Teflon-PP composite membrane in the immersion tests. In PMP composite membrane (Figure 2A and B), the thickness of the PMP dense layer increases evidently after the immersion test, most likely due to the swelling of PMP by the [Bmim][TCM]. This clearly shows that the PMP membrane is not suitable for this membrane contactor application due to the change of the membrane nature and the lack of long-term stability in the IL absorbent.

Figure 2C and D presents the SEM image of the Teflon-PP composite membranes before and after the immersion tests. No obvious changes can be found, suggesting that the Teflon-coated composite membrane can be a suitable membrane for the application.
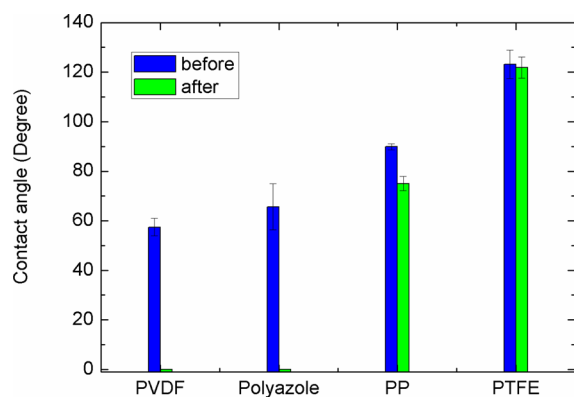
Figure 2. PMP composite membrane (A,B) and Teflon-PP (C,D) membrane before (left) and after (right) the immersion tests.

According to the SEM images, except for the PMP composite membrane, five other tested membranes have both good compatibility and thermal stability in [Bmim][TCM]. However, as the color changed from white to transparent during the immersion, the porous polyazole and PVDF membrane suffered IL penetration.

Contact Angle. According to the Young–Laplace equation, a contact angle between the porous membrane and liquid absorbent higher than 90° is a prerequisite for avoiding membrane wetting.[39] Therefore, the contact angles between the [Bmim][TCM] and the four porous membranes that showed good compatibility were measured by using the static sessile drop method. For each membrane, a fresh sample and a sample immersed in [Bmim][TCM] at 100 °C for 6 h were used to investigate the influence of [Bmim][TCM] on the surface wettability.

The color of the PVDF and polyazole membranes gradually changed from white to transparent when they were soaked in [Bmim][TCM] even at room temperature, suggesting a possible spontaneous penetration of [Bmim][TCM] into the membrane pores. This was confirmed by the contact angle tests. Untreated PVDF and polyazole membranes showed a contact angle of around 57° and 65°, respectively (Figure 3),
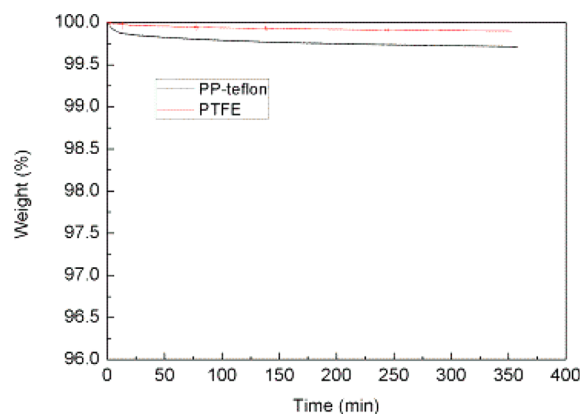
but it tended to reduce gradually and became negligible in a couple of minutes; this happens only when the pores on the surface are occupied by the same liquid. It is thus concluded that PVDF and polyazole membranes are easily wetted in ILs and not suitable as membrane interface in the membrane contactor in this process.

Significantly higher contact angle and less reduction after the immersion test were obtained with the porous PP and PTFE membranes as can be seen in Figure 3. The initial contact angle measured on the neat PP polymer was 90°, whereas in the case of PTFE it was even higher and corresponded to 123° (Figure 3). However, the sample undergone IL at high temperatures shows an increase in their wettability: the contact angle of the PP membrane reduced approximately 14.8°, becoming far below 90°; whereas for the PTFE membrane, the contact angle was found to be still 122° with a reduction of only about 1.2°. The results suggest that among the four porous membrane candidates only the porous PTFE membrane is suitable for the designed application. PP porous membrane cannot be used due to the potential membrane wetting. However, with a good chemical stability with ILs, PP can be a suitable porous support in preparing composite membranes.

The contact angle test of Teflon-PP composite membranes was conducted, where a value equal to 102° was observed, which is much higher than the pristine PP porous support and quite close to the contact angle of the dense Teflon membrane (~105°), suggesting that the PP is fully covered by the Teflon coating. According to the good stability and compatibility observed, the Teflon-PP composite membrane is selected as the nonporous composite membrane for further study.

3.1.2. Thermal Stability Evaluation. It is important that the membrane materials have good thermal stability to operate at elevated temperatures in this work. From the morphological analysis carried out with the SEM investigation, it was found that after the treatment of [Bmim][TCM] at 100 °C for 6 h, no morphology changes or pore collapse were observed for the porous PTFE membrane and the Teflon-PP composite membrane, suggesting both good thermal stability and good chemical stability in these two membranes.

Thermal gravimetric analysis (TGA) was applied to further evaluate the thermal stability of the selected porous PTFE membrane and nonporous Teflon-PP composite membrane. As can be seen from Figure 4, both membranes showed excellent thermal stabilities at 100 °C. For the PTFE membrane, the weight loss in 6 h is less than 0.1%, denoting that this membrane is stable under the studied temperature. It was a

Figure 3. Contact angle of the PVDF, Polyazole, PP, and PTFE membranes before and after the treatment of [Bmim][TCM] at 100 °C for 6 h.

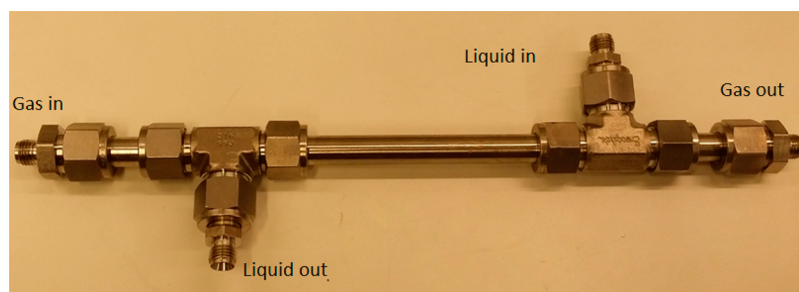**Figure 4.** Thermal stability test of Teflon-PP and PTFE, 100 °C, 6 h.

E

Figure 5. Optical image of the membrane module.

little different for the Teflon-PP membrane; a decrease in the first 20 min occurred, possibly due to the evaporation of the residual solvent in the membrane. Nevertheless, the weight loss during the remaining 5 h was only around 0.2%, indicating that this membrane is also stable at this temperature. These two TGA results agree well with the morphology investigations.

3.2. Separation Performances. On the basis of the compatibility screening, two membranes are considered suitable for the preparation of membrane modules in the membrane contactor: the porous PTFE membrane ($T_g \approx -100$ °C[40]) and the Teflon-PP composite membrane (AF 2400 $T_g \approx 240$ °C, PP $T_g \approx 13$ °C). The two membranes were therefore chosen and made as hollow fiber modules for further investigation.

A number of hollow fiber membranes were placed in a small filter paper with holes and inserted into a half-inch stainless steel tube. The potting material (high temperature two-composite epoxy, purchased from Aremco, U.S.) was injected onto the filter paper to form a solid plug. The same procedure was repeated on the opposite side of the membrane module. Figure 5 shows the optical image of the membrane module.

In Table 1 are reported the specifications of the membrane module prepared for the present study.

Table 1. Specifications of the Membrane Module Used in This Study

parameter	PTFE	Teflon-PP
membrane module length (mm)	300	250
effective membrane length (mm)	260	210
module diameter (mm)	10.2	10.2
membrane i.d. (mm)	1.01	0.2
membrane o.d. (mm)	1.39	0.3
number of membranes	4	15
dense layer thickness (um)		1
total membrane area (m^2)	0.0296	0.0367

It is worth mentioning that the two hollow fiber membranes have very different fiber sizes. The PTFE hollow fiber membrane is much larger in diameter as compared to the PP hollow fibers due to the limitation of the processability of PTFE as a polymer. As compared to the PTFE membrane, the Teflon-PP composite membrane can offer a higher surface area-to-volume ratio because of its smaller membrane diameter.

The membrane modules were installed inside the membrane contactor rig to evaluate the separation performances as well as the influences of the gas flow rate and the operation pressure on the gas separation performances. In view of the volumetric limitation of the piston accumulator (2 L) used to inject the absorbent into the test rig and the minimum stabilization time of the system (~30 min), the liquid flow was kept at 20 mL

min^{-1} for all of the performed tests. All of the CO$_2$ flux reported in the present work is estimated from the average value of at least two tests with an error lower than 10%.

3.2.1. Effect of Operation Pressure. The CO$_2$ flux values at pressures up to 20 bar for the porous PTFE and Teflon-PP composite membrane contactors are shown in Figure 6.

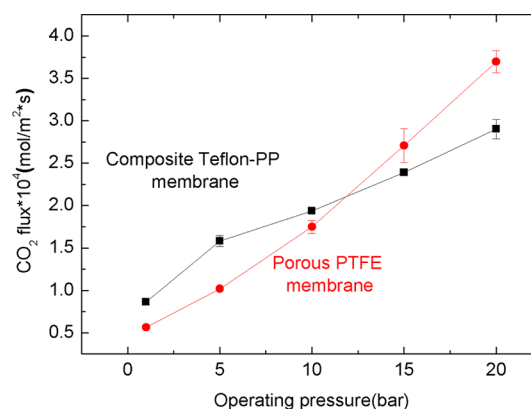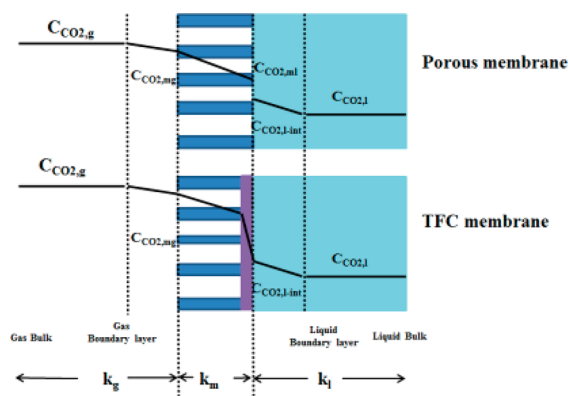**Figure 6.** Effect of operative pressure on the CO$_2$ separation performances, CO$_2$ flux (operating conditions: Q_{liquid} = 20 mL min^{-1}, Q_{gas} = 100 mL min^{-1}, T = 80 °C).
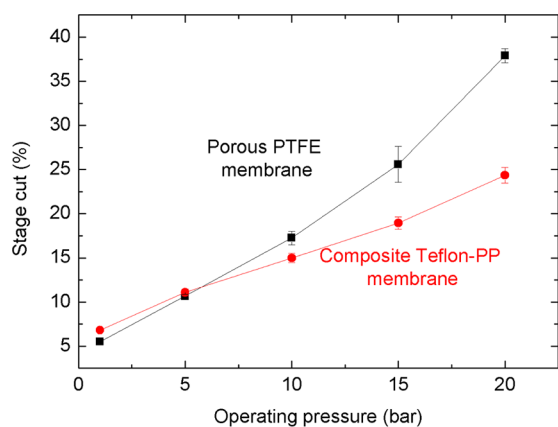
As expected, in both membrane contactors, the CO$_2$ flux was greatly enhanced by increasing the operating pressure due to the larger CO$_2$ driving forces at a higher CO$_2$ partial pressure. Surprisingly, at 1 bar the porous PTFE membrane showed a lower CO$_2$ flux (0.56 × 10^{-4} mol m^{-2} s^{-1}) than the Teflon-PP nonporous TFC composite membrane (0.86 × 10^{-4} mol m^{-2} s^{-1}). However, the CO$_2$ flux of the PTFE membrane contactor was greatly enhanced and became higher than that of the Teflon-PP membrane contactor by increasing the operating pressure to 20 bar, with values corresponding to 3.70 × 10^{-4} and 2.90 × 10^{-4} mol m^2 s^{-1}, respectively. Increasing the operative pressure seemed more effective in enhancing the CO$_2$ flux for the porous PTFE membrane than the Teflon-PP composite membrane. The contribution of the mass transfer resistance in membrane phase and liquid phase at different pressure range may explain this trend (as shown in Figure 7). Generally, if no chemical reaction is involved, the liquid side mass transfer resistance dominates the overall mass transfer in a membrane contactor.[41] Because of the high CO$_2$ permeability (a CO$_2$ permeability of 3900 Barrer was reported for Teflon AF 2400 thin film membrane with thickness of 1.5 μm at 20 bar and 35 °C[42]), the presence of the top dense Teflon AF 2400 layer adds only a small fraction of the mass transfer resistance in the membrane phase. At low pressures, the better dispersion of gases into the liquid phase through the smaller Teflon-PP fibers

Figure 7. Mass-transfer regions and resistance-in-series in membrane contactors based on porous membranes and composite membranes.

(0.3 mm) may enhance the liquid phase mass transfer and results in a high CO_2 flux. However, due to the ionic nature of the [Bmim][TCM], the electrostatic attraction between the IL and Teflon-PP membrane may have forced the membrane to stick together as a bunch of fibers (this phenomenon was observed after the test), reducing the effective gas/liquid interface and consequently CO_2 flux, specifically at high operation pressures. On the other hand, as the mass transfer resistance in the porous membrane is relatively less as compared to a nonporous membrane, increasing operating pressure is more effective in enhancing CO_2 flux in the porous PTFE membrane contactor.
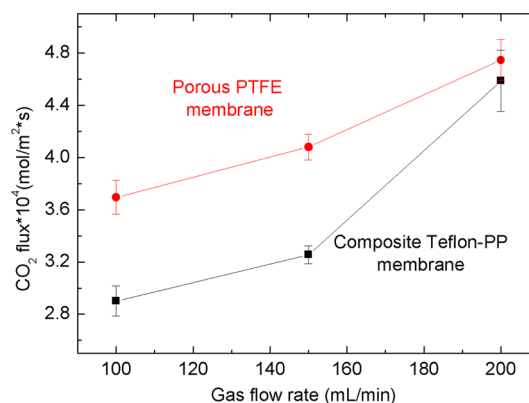
The stage-cut values of both PTFE and Teflon-PP composite membrane contactors at various pressures were calculated and plotted in Figure 8. As mentioned earlier, due to the limitation

Figure 8. Effect of operative pressure on the CO_2 separation performances, stage-cut (operating conditions: Q_{liquid} = 20 mL min^{-1}, Q_{gas} = 100 mL min^{-1}, T = 80 °C).

of the piston accumulator used in this study, the liquid flow rate was fixed to be 20 mL min^{-1}, but a much higher gas flow rate (100−200 mL min^{-1}) must be applied to reduce the experimental error. The high gas/liquid flow ratio and the limited CO_2 solubility in the solvent resulted in a small variation between the feed and retentate gas composition, especially at low operating pressure conditions. As expected, low stage-cuts were obtained at low pressures, and the stage-cut increases notably with the increase of operating pressures for both cases due to the significant increase of the CO_2 solubility in the IL solvent at higher pressures.

3.2.2. Effect of the Gas Flow Rate. The effect of the gas flow rate on CO_2 flux was studied. Increasing gas flow rate usually enhances mass transfer in the gas phase and lead to a higher CO_2 flux in a membrane contactor.[32,43] Experimental results in this work agree well with this expected trend, but the effects of gas flow rate on porous and nonporous membranes are different, as can be seen in Figure 9. In the porous PTFE
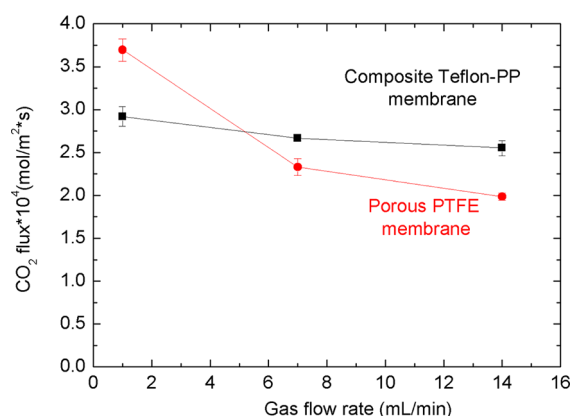

Figure 9. Effect of gas flow rate on the CO_2 separation performances (operating conditions: Q_{liquid} = 20 mL min^{-1}, T = 80 °C, p = 20 bar).

membrane contactor, the CO_2 flux increased from 3.70×10^{-4} to 4.86×10^{-4} mol m^{-2} s^{-1} when the gas flow rate increased from 100 to 200 mL min^{-1}. A higher gas flow rate can reduce the gas-phase resistance, and also partially reduce the potential of membrane wetting in the porous membrane, which may result in a better mass transfer through the membrane. In the nonporous Teflon-PP composite membrane contactor, the CO_2 flux was enhanced from 2.90×10^{-4} to 4.75×10^{-4} mol m^{-2} s^{-1} as well. It is interesting that the CO_2 flux at a low gas flow rate in the nonporous composite membrane is much lower than that in a porous membrane contactor, but at a high gas flow both membranes show similar CO_2 flux. Increasing gas flow is more effective in enhancing mass transfer in the nonporous composite membrane contactor. Theoretically, the mass transfer resistance in the gas phase only contributes a small portion to the overall mass transfer resistance, and increasing gas-phase flow rate has a limited impact on the overall mass transfer coefficient and CO_2 flux. However, in the present study, increasing gas flow rate effectively enhances the CO_2 flux. Except for the improved gas-phase mass transfer, the higher gas flow rate may have partially reduced the membrane wetting or membrane fiber cohesive packing, and hence increased the CO_2 flux.

3.2.3. Long-Term Stability Performances. It is commonly reported that in most porous membrane contactors, the membrane pores will be gradually wetted over time and the membrane mass transfer resistance increases greatly, leading to significant reductions in CO_2 flux.[44,45] In this work, the long-term stability of the porous PTFE membrane contactor and Teflon-PP composite membrane contactor was studied by comparing the CO_2 fluxes of the two membranes conditioned over 14 days, as shown in Figure 10.

For safety reasons and due to the limited amount of ionic liquids, the long-term stability test was not carried through a continuous operation. To investigate the long-term influence of the ILs at the operating temperature, the membrane module was first tested at 80 °C and 20 bar for about 2 h, and then soaked in [Bmim][TCM] at 80 °C and 1 bar before the second
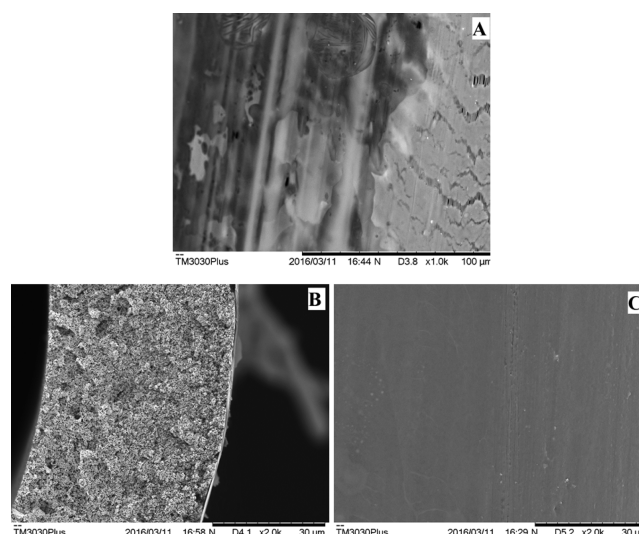
Figure 10. Long-term stability performances of the PTFE and Teflon-PP membrane contactors (operating conditions: Q_{liquid} = 20 mL min^{-1}, T = 80 °C, p = 20 bar).

Figure 11. PTFE porous membrane surface (A) and Teflon-PP composite membrane cross section (B) and surface (C) after the long-term stability test.

and third tests were performed. As shown in Figure 10, a 50% reduction in the CO_2 flux through the PTFE membrane can be observed after the first week of operation, but a smaller reduction was obtained during the second week. The decline of flux is most likely due to the morphological rearrangements and pore wetting by the ILs. On the other hand, even though the Teflon-PP composite membrane showed a lower initial CO_2 flux as compared to the porous PTFE, a more stable operation was achieved through the 2-week investigation. The flux reduction was less than 15% of the initial value after 2 weeks, and it decreased and became evidently slower: the flux reduction was only around 1% during the second week, which is within the range of the experimental error. It is believed that the reduction of CO_2 flux in the Teflon-PP composite membrane resulted from the physical aging of the thin Teflon AF 2400 layer and the CO_2 flux will be gradually stabilized.[28] According to the literature for a Teflon membrane, the aging effect took place mainly during the first days of operation, and no further decrease in performance was observed.[28]

The membrane morphologies after the long-term stability test were also investigated by SEM shown in Figure 11.

As shown in Figure 1E and F, no obverse changes can be found from the PTFE membrane after being soaked in [Bmim][TCM] at 100 °C for 6 h at atmospheric pressure. However, in Figure 11A, it is clearly shown that the PTFE membrane surface was partially destroyed by [Bmim][TCM] after the long-term stability test after operation at 20 bar, where part of the PTFE membrane surface was removed by IL and the surface morphology was changed (the left-hand part in Figure 11A). The high operating pressure and the possible pore wetting as well as the flowing IL seem more aggressive to the PTFE membrane. The significant change in membrane surface also explains the big differences in the CO_2 flux over time. Conversely, the Teflon-PP composite membranes are more stable in the long-term stability test; no obvious changes can be found from both the surface and the cross section, as shown in Figure 11B and C. Neither liquid penetration nor top layer swelling were observed in this membrane, denoting a superior stability property of the Teflon-PP composite membrane in [Bmim][TCM] than the porous PTFE membrane for this process, which agrees well with the more stable separation performance. The SEM images before and after the stability tests in Figure 11 and the results in Figure 10 confirm that the

Teflon-PP composite membrane has better long-term stability in the IL membrane contactor as compared to the porous PTFE membrane.

4. CONCLUSION

On the basis of the screening of six polymeric membranes (four porous membranes and two thin film composite membranes) for the preparation of a membrane module in a membrane contactor for precombustion CO_2 capture, two membranes, that is, the porous PTFE membrane and nonporous Teflon-PP composite membrane, were chosen due to their superior thermal stability, good chemical stability, and better compatibility with the selected IL ([Bmim][TCM]). The CO_2 capture separation performances of the two membrane contactors using the selected hollow fiber membranes were investigated at 80 °C and 20 bar. The effects of operating parameters such as operation pressure and gas flow rate were investigated, and it was found that the operation pressure can greatly promote the CO_2 flux in both porous PTFE membrane and nonporous composite Teflon-PP membrane, with a more significant effect on the porous membrane. A higher gas flow rate can result in a higher CO_2 flux in both types of membrane, while the porous PTFE membrane contactor exhibits a higher CO_2 flux and the Teflon-PP composite membrane contactor presents better long-term stability. The [Bmim][TCM] can gradually attack the PTFE membrane in high-pressure conditions and partially dissolve the membrane material.

The Teflon-PP composite membrane is considered more suitable for application. However, surprisingly, when the Teflon-PP composite membrane was used, the cohesive packing of the membrane fibers occurred, which reduces the effective membrane area. In a future study, membrane surface modification and employment of spacers in the membrane modules can be used to reduce membrane cohesive packing. The use of blend ILs with other liquid absorbent can be another approach. The membrane module design and operation parameters also can be further optimized to achieve an efficient separation.

■ AUTHOR INFORMATION

Corresponding Author
*Tel.: +47 73594112. E-mail: deng@nt.ntnu.no.
Notes
The authors declare no competing financial interest.

■ REFERENCES

(1) Yang, H.; Xu, Z.; Fan, M.; Gupta, R.; Slimane, R. B.; Bland, A. E.; Wright, I. Progress in carbon dioxide separation and capture: A review. *J. Environ. Sci.* **2008**, *20* (1), 14−27.

(2) Li, B. Y.; Duan, Y. H.; Luebke, D.; Morreale, B. Advances in CO2 capture technology: A patent review. *Appl. Energy* **2013**, *102*, 1439−1447.

(3) Mansourizadeh, A.; Ismail, A. F. Hollow fiber gas-liquid membrane contactors for acid gas capture: A review. *J. Hazard. Mater.* **2009**, *171* (1−3), 38−53.

(4) Luis, P.; Van der Bruggen, B.; Van Gerven, T. Non-dispersive absorption for CO2 capture: from the laboratory to industry. *J. Chem. Technol. Biotechnol.* **2011**, *86* (6), 769−775.

(5) Zhao, S.; Feron, P. H. M.; Deng, L.; Favre, E.; Chabanon, E.; Yan, S.; Hou, J.; Chen, V.; Qi, H. Status and progress of membrane contactors in post-combustion carbon capture: A state-of-the-art review of new developments. *J. Membr. Sci.* **2016**, *511*, 180−206.

(6) Dindore, V. Y.; Brilman, D. W. F.; Geuzebroek, F. H.; Versteeg, G. F. Membrane-solvent selection for CO2 removal using membrane gas-liquid contactors. *Sep. Purif. Technol.* **2004**, *40* (2), 133−145.

(7) Constantinou, A.; Barrass, S.; Gavriilidis, A. CO2 Absorption in Polytetrafluoroethylene Membrane Microstructured Contactor Using Aqueous Solutions of Amines. *Ind. Eng. Chem. Res.* **2014**, *53* (22), 9236−9242.

(8) Iliuta, I.; Bougie, F.; Iliuta, M. C. CO2 Removal by Single and Mixed Amines in a Hollow-Fiber Membrane Module-Investigation of Contactor Performance. *AIChE J.* **2015**, *61* (3), 955−971.

(9) Wang, Z.; Fang, M. X.; Yan, S. P.; Yu, H.; Wei, C. C.; Luo, Z. Y. Optimization of Blended Amines for CO2 Absorption in a Hollow-Fiber Membrane Contactor. *Ind. Eng. Chem. Res.* **2013**, *52* (34), 12170−12182.

(10) Kosaraju, P.; Kovvali, A. S.; Korikov, A.; Sirkar, K. K. Hollow Fiber Membrane Contactor Based CO2 Absorption−Stripping Using Novel Solvents and Membranes. *Ind. Eng. Chem. Res.* **2005**, *44* (5), 1250−1258.

(11) Paul, S.; Ghoshal, A. K.; Mandal, B. Removal of CO2 by single and blended aqueous alkanolamine solvents in hollow-fiber membrane contactor: Modeling and simulation. *Ind. Eng. Chem. Res.* **2007**, *46* (8), 2576−2588.

(12) Gouedard, C.; Picq, D.; Launay, F.; Carrette, P. L. Amine degradation in CO2 capture. I. A review. *Int. J. Greenhouse Gas Control* **2012**, *10*, 244−270.

(13) Zhang, X. P.; Zhang, X. C.; Dong, H. F.; Zhao, Z. J.; Zhang, S. J.; Huang, Y. Carbon capture with ionic liquids: overview and progress. *Energy Environ. Sci.* **2012**, *5* (5), 6668−6681.

(14) Ramdin, M.; de Loos, T. W.; Vlugt, T. J. H. State-of-the-Art of CO₂ Capture with Ionic Liquids. *Ind. Eng. Chem. Res.* **2012**, *51* (24), 8149−8177.

(15) Albo, J.; Luis, P.; Irabien, A. Carbon Dioxide Capture from Flue Gases Using a Cross-Flow Membrane Contactor and the Ionic Liquid 1-Ethyl-3-methylimidazolium Ethylsulfate. *Ind. Eng. Chem. Res.* **2010**, *49* (21), 11045−11051.

(16) Albo, J.; Irabien, A. Non-dispersive absorption of CO₂ in parallel and cross-flow membrane modules using EMISE. *J. Chem. Technol. Biotechnol.* **2012**, *87* (10), 1502−1507.

(17) Jie, X. M.; Chau, J.; Obuskovic, G.; Sirkar, K. K. Enhanced Pressure Swing Membrane Absorption Process for CO₂ Removal from Shifted Syngas with Dendrimer-Ionic Liquid Mixtures as Absorbent. *Ind. Eng. Chem. Res.* **2014**, *53* (8), 3305−3320.

(18) Gomez-Coma, L.; Garea, A.; Irabien, A. Non-dispersive absorption of CO₂ in [emim][EtSO₄] and [emim][Ac]: Temperature influence. *Sep. Purif. Technol.* **2014**, *132*, 120−125.

(19) Luis, P.; Garea, A.; Irabien, A. Zero solvent emission process for sulfur dioxide recovery using a membrane contactor and ionic liquids. *J. Membr. Sci.* **2009**, *330* (1−2), 80−89.

(20) Ortiz, A.; Gorri, D.; Irabien, A.; Ortiz, I. Separation of propylene/propane mixtures using Ag+-RTIL solutions. Evaluation and comparison of the performance of gas-liquid contactors. *J. Membr. Sci.* **2010**, *360* (1−2), 130−141.

(21) Albo, J.; Luis, P.; Irabien, A. Absorption of coal combustion flue gases in ionic liquids using different membrane contactors. *Desalin. Water Treat.* **2011**, *27* (1−3), 54−59.

(22) Lu, J. G.; Lu, C. T.; Chen, Y.; Gao, L.; Zhao, X.; Zhang, H.; Xu, Z. W. CO₂ capture by membrane absorption coupling process: Application of ionic liquids. *Appl. Energy* **2014**, *115*, 573−581.

(23) Mulukutla, T.; Chau, J.; Singh, D.; Obuskovic, G.; Sirkar, K. K. Novel membrane contactor for CO2 removal from flue gas by temperature swing absorption. *J. Membr. Sci.* **2015**, *493*, 321−328.

(24) Mosadegh-Sedghi, S.; Rodrigue, D.; Brisson, J.; Iliuta, M. C. Wetting phenomenon in membrane contactors − Causes and prevention. *J. Membr. Sci.* **2014**, *452*, 332−353.

(25) Nguyen, P. T.; Lasseuguette, E.; Medina-Gonzalez, Y.; Remigy, J. C.; Roizard, D.; Favre, E. A dense membrane contactor for intensified CO2 gas/liquid absorption in post-combustion capture. *J. Membr. Sci.* **2011**, *377* (1−2), 261−272.

(26) AlSaffar, H. B.; Ozturk, B.; Hughes, R. A comparison of porous and non-porous gas-liquid membrane contactors for gas separation. *Chem. Eng. Res. Des.* **1997**, *75* (A7), 685−692.

(27) Scholes, C. A.; Qader, A.; Stevens, G. W. Kentish, S. E. Membrane Gas-Solvent Contactor Pilot Plant Trials of CO2 Absorption from Flue Gas. *Sep. Sci. Technol.* **2014**, *49* (16), 2449−2458.

(28) Scholes, C. A.; Kentish, S. E.; Stevens, G. W.; deMontigny, D. Comparison of thin film composite and microporous membrane contactors for CO2 absorption into monoethanolamine. *Int. J. Greenhouse Gas Control* **2015**, *42*, 66−74.

(29) Chen, H. Z.; Thong, Z. W.; Li, P.; Chung, T. S. High performance composite hollow fiber membranes for CO2/H-2 and CO2/N-2 separation. *Int. J. Hydrogen Energy* **2014**, *39* (10), 5043−5053.

(30) Dai, Z. D.; Noble, R. D.; Gin, D. L.; Zhang, X. P.; Deng, L. Y. Combination of ionic liquids with membrane technology: A new approach for CO2 separation. *J. Membr. Sci.* **2016**, *497*, 1−20.

(31) Zubeir, L. F.; Romanos, G. E.; Weggemans, W. M. A.; Iliev, B.; Schubert, T. J. S.; Kroon, M. C. Solubility and Diffusivity of CO2 in the Ionic Liquid 1-Butyl-3-methylimidazolium Tricyanomethanide within a Large Pressure Range (0.01 to 10 MPa). *J. Chem. Eng. Data* **2015**, *60* (6), 1544−1562.

(32) Wang, R.; Zhang, H. Y.; Feron, P. H. M.; Liang, D. T. Influence of membrane wetting on CO2 capture in microporous hollow fiber membrane contactors. *Sep. Purif. Technol.* **2005**, *46* (1−2), 33−40.

(33) Yokozeki, A.; Shiflett, M. B.; Junk, C. P.; Grieco, L. M.; Foo, T. Physical and Chemical Absorptions of Carbon Dioxide in Room-Temperature Ionic Liquids. *J. Phys. Chem. B* **2008**, *112* (51), 16654−16663.

(34) Rahbari-Sisakht, M.; Ismail, A. F.; Rana, D.; Matsuura, T. Carbon dioxide stripping from diethanolamine solution through porous surface modified PVDF hollow fiber membrane contactor. *J. Membr. Sci.* **2013**, *427*, 270−275.

(35) Chabanon, E.; Bounaceur, R.; Castel, C.; Rode, S.; Roizard, D.; Favre, E. Pushing the limits of intensified CO2 post-combustion

capture by gas-liquid absorption through a membrane contactor. *Chem. Eng. Process.* **2015**, *91*, 7−22.

(36) Lv, Y. X.; Yu, X. H.; Tu, S. T.; Yan, J. Y.; Dahlquist, E. Experimental studies on simultaneous removal of CO2 and SO2 in a polypropylene hollow fiber membrane contactor. *Appl. Energy* **2012**, *97*, 283−288.

(37) Maab, H.; Francis, L.; Al-Saadi, A.; Aubry, C.; Ghaffour, N.; Amy, G.; Nunes, S. P. Synthesis and fabrication of nanostructured hydrophobic polyazole membranes for low-energy water recovery. *J. Membr. Sci.* **2012**, *423*, 11−19.

(38) Makhloufi, C.; Lasseuguette, E.; Remigy, J. C.; Belaissaoui, B.; Roizard, D.; Favre, E. Ammonia based CO2 capture process using hollow fiber membrane contactors. *J. Membr. Sci.* **2014**, *455*, 236−246.

(39) Garcia-Payo, M. C.; Izquierdo-Gil, M. A.; Fernandez-Pineda, C. Wetting study of hydrophobic membranes via liquid entry pressure measurements with aqueous alcohol solutions. *J. Colloid Interface Sci.* **2000**, *230* (2), 420−431.

(40) Calleja, G.; Jourdan, A.; Ameduri, B.; Habas, J. P. Where is the glass transition temperature of poly(tetrafluoroethylene)? A new approach by dynamic rheometry and mechanical tests. *Eur. Polym. J.* **2013**, *49* (8), 2214−2222.

(41) Mavroudi, M.; Kaldis, S. P.; Sakellaropoulos, G. P. A study of mass transfer resistance in membrane gas-liquid contacting processes. *J. Membr. Sci.* **2006**, *272* (1−2), 103−115.

(42) Tiwari, R. R.; Smith, Z. P.; Lin, H.; Freeman, B. D.; Paul, D. R. Gas permeation in thin films of "high free-volume" glassy perfluoropolymers: Part II. CO2 plasticization and sorption. *Polymer* **2015**, *61*, 1−14.

(43) Zhang, H. Y.; Wang, R.; Liang, D. T.; Tay, J. H. Modeling and experimental study of CO2 absorption in a hollow fiber membrane contactor. *J. Membr. Sci.* **2006**, *279* (1−2), 301−310.

(44) Zhang, H. Y.; Wang, R.; Liang, D. T.; Tay, J. H. Theoretical and experimental studies of membrane wetting in the membrane gas-liquid contacting process for CO2 absorption. *J. Membr. Sci.* **2008**, *308* (1−2), 162−170.

(45) Mosadegh-Sedghi, S.; Rodrigue, D.; Brisson, J.; Iliuta, M. C. Wetting phenomenon in membrane contactors - Causes and prevention. *J. Membr. Sci.* **2014**, *452*, 332−353.